Check for updates

ASCE

Coupled Creep-Damage-Plasticity Model for Concrete under Long-Term Loading

Xiaodan Ren, Ph.D.[1]; Qing Wang[2]; Roberto Ballarini, Ph.D., P.E., F.ASCE[3]; and Xiangling Gao, Ph.D.[4]

Abstract: A damage-plasticity model is extended to account for the effects of simultaneously occurring stiffness degradation, residual deformation, and creep. Assuming the additivity of small strains, the model combines damage mechanics, plasticity theory, and an improved version of the ACI model to characterize creep at low stress levels. The coupling between damage and creep produced by medium and high stress levels is accounted for by introducing a damage-dependent influence function. An explicit numerical algorithm is developed to implement the proposed model in the simulations of structural response. The proposed model is systematically validated by comparing its results with experimental data, suggesting that it offers promise for capturing the long-term mechanical behavior of reinforced concrete structures.
DOI: 10.1061/(ASCE)EM.1943-7889.0001748. © *2020 American Society of Civil Engineers.*

Author keywords: Concrete; Damage-plasticity model; Linear creep; Nonlinear creep.

Downloaded from ascelibrary.org by University of Houston on 08/11/20. Copyright ASCE. For personal use only; all rights reserved.

Introduction

Creep of concrete structures is an important issue in the field of civil engineering. Its detrimental effects on safety, durability, and functionality include a gradual increase of deformation, potentially dangerous stress redistribution phenomena and long-term reduction of compressive strength. Quantitatively accurate calculations of creep are therefore essential for structural analysis and design.

Although the physical mechanisms responsible for creep are still being investigated by the mechanics of concrete community, experimental data have led to a consensus that concrete is susceptible to three kinds of creep; linear, nonlinear, and tertiary. Within the linear range, corresponding to stress levels below approximately 40% of the concrete strength, the material is not significantly damaged, and the response can be described by the linear theory of viscoelasticity; creep strain is proportional to stress. For medium and high stress levels, in the range of 40%–70% of concrete strength, cracking phenomena renders the creep response nonlinear; creep strain is no longer proportional to stress. In this state, there is an intimate coupling between the level of stress and the evolution of creep. For higher stress levels, experimental results (Carol and Murcia 1989; Omar et al. 2009) suggest a rapidly increasing rate of creep up to failure. This so-called tertiary creep is attributed to the unstable development of cracks during the load holding process. The scope of this paper is limited to the study of the first two stages of concrete creep. Its main contribution is the presentation of a new nonlinear creep model where a damage-dependent influence function is introduced to account for the coupling between damage and creep, and the combining of linear and nonlinear creep behaviors.

Simulations of the mechanical behavior of concrete under long-term loading conditions necessitates models that consider simultaneously occurring creep and damage phenomena. Significant progress has been made along these lines. In the coupled damage and creep models (Mazzotti and Savoia 2003; Challamel et al. 2005; Reviron et al. 2007; Benboudjema and Torrenti 2008), a generalized Maxwell or Kelvin model is adopted to reproduce the creep behavior, and a continuum damage model is used to take into account the initiation and growth of microcracks. In the solidification-microprestress-microplane theory (Luzio and Cusatis 2013), the combination of the microplane model and microprestress-solidification model is formulated to incorporate damage and creep behavior into a united framework. In other studies, a time-dependent extension of damage is proposed. The temporal variable, namely the effective creep Poisson's ratio of damaged concrete, is introduced in the model of Li (1994) to consider the effects of creep in the lateral direction.

As previously stated, under medium and high stress levels, creep strain is associated with the growth and developing of microcracks (Mazzotti and Savoia 2003; Neville 1971; Proust and Prons 2001). Few analytic and computational models are available that account for the combined effects of nonlinear creep and damage. According to Bažant and Prasannan (1989), the nonlinear dependence of creep with respect to stress is introduced by multiplying the current creep rate by a nondimensional function. This function is related to the current stress and does not depend on the previous stress history. The model of Mazzotti and Savoia (2003) introduces the concept of effective strain to replace the equivalent strain for damage evaluation. Based on the assumption that the contribution of the elastic strain to the damage evolution is greater than that of the creep strain, the effective strain is written as the sum of the elastic strain and a fraction of creep strain. Similar approaches were adopted by others (Omar et al. 2003; Reviron et al. 2007). The physical model proposed by Ruiz et al. (2007), which was experimentally validated, assumes that nonlinear creep strains are due to microcracks

[1]Associate Professor, College of Civil Engineering, Tongji Univ., 1239 Siping Rd., Shanghai 200092, PR China. Email: rxdtj@tongji.edu.cn

[2]Ph.D. Student, College of Civil Engineering, Tongji Univ., 1239 Siping Rd., Shanghai 200092, PR China. Email: 1323604728@qq.com

[3]Thomas and Laura Hsu Professor and Chair, Dept. of Civil and Environmental Engineering, Univ. of Houston, N127 Engineering Bldg. 1, Houston, TX 77204-4003. Email: rballarini@uh.edu

[4]Associate Professor, College of Civil Engineering, Tongji Univ., 1239 Siping Rd., Shanghai 200092, PR China (corresponding author). Email: gaoxl@tongji.edu.cn

Note. This manuscript was submitted on June 24, 2019; approved on October 9, 2019; published online on February 21, 2020. Discussion period open until July 21, 2020; separate discussions must be submitted for individual papers. This paper is part of the ***Journal of Engineering Mechanics***, © ASCE, ISSN 0733-9399.

and defects within the material volume. The nonlinear relation between creep strain and the stress level is introduced through a stress-dependent creep coefficient. This nonlinear approach is simple but not suitable for the multiaxial stress state.

In the present paper, a coupled creep-damage-plasticity model for concrete under long-term loading conditions is presented. It takes into account creep, plasticity, and damage. Based on the small strain additivity assumption, the energy-based framework of the damage-plasticity model proposed by Wu et al. (2006) and Ren et al. (2015) is adopted here. The creep behavior is described by extending a modified ACI model to multidimensional stress states. Nonlinear creep is introduced by multiplying the current creep strain by a damage-dependent influence function that couples damage and creep. The model is implemented numerically and validated by comparing its results with experimental data from: concrete subjected to uniaxial compression, reinforced concrete beams under transverse loading, and reinforced concrete columns under compressive loading. These numerical results are in good agreement with the experimental results, and give confidences that the model is capable of charactering both linear and nonlinear creep deformations.

Coupled Creep-Damage-Plasticity Model

The constitutive relationship formulated in the present paper is based on the assumption of strain additivity. Assuming small strains, the total strain ($\boldsymbol{\varepsilon}$) is comprised of three components; the elastic (instantaneous and recoverable) strain ($\boldsymbol{\varepsilon}^e$), plastic (instantaneous and irreversible) strain ($\boldsymbol{\varepsilon}^p$) and creep (time dependent) strain ($\boldsymbol{\varepsilon}^c$)

$$\boldsymbol{\varepsilon} = \boldsymbol{\varepsilon}^e + \boldsymbol{\varepsilon}^p + \boldsymbol{\varepsilon}^c \tag{1}$$

For typical short-term loading conditions, or more precisely for instantaneous loading conditions, the third term on the right-hand side of Eq. (1) is nearly equal to zero. The additivity assumption could be represented by the rheological model depicted in Fig. 1, for which the components are coupled in series and thus equally stressed.

The strain additivity assumption, which has also been referred to as the strain splitting assumption, is the basis of several constitutive models of concrete. (Rabier 1989; Bažant and Prasannan 1989; Mazzotti and Savoia 2003; Wu et al. 2006; Voyiadjis et al. 2008).

According to the established concept in the damage mechanics literature (Lemaitre and Chaboche 1990; Voyiadjis et al. 2008; Vayiadjis and Kattan 2009), the applied nominal stress ($\boldsymbol{\sigma}$) is mapped into the effective stress ($\boldsymbol{\sigma}$) by the fourth-order damage effect tensor $\mathbb{M}$

$$\bar{\boldsymbol{\sigma}} = \mathbb{M}:\boldsymbol{\sigma} \tag{2}$$

In this work, the energy-based framework of damage-plasticity theory proposed by Wu et al. (2006) and Ren et al. (2015) is adopted to describe the degradation of concrete stiffness due to the development of microcracks and the irrecoverable instantaneous plastic deformation simultaneously. The constitutive relationship under conventional short-term loading condition can be expressed as follows

$$\boldsymbol{\sigma} = (\mathbb{I} - \mathbb{D}):\bar{\boldsymbol{\sigma}} \tag{3}$$

where $\mathbb{I}$ = fourth-order identity tensor, and $\mathbb{D}$ = fourth-order damage tensor which accounts for the degradation of the effective stress. By comparing Eq. (3) with Eq. (2), the damage effect tensor is expressed as follows

$$\mathbb{M} = (\mathbb{I} - \mathbb{D})^{-1} \tag{4}$$

Further, based on the strain additivity assumption, the effective stress under long-term loading condition could be represented by

$$\bar{\boldsymbol{\sigma}} = \mathbb{E}_0:\boldsymbol{\varepsilon}^e = \mathbb{E}_0:(\boldsymbol{\varepsilon} - \boldsymbol{\varepsilon}^p - \boldsymbol{\varepsilon}^c) \tag{5}$$

where $\mathbb{E}_0$ = fourth-order initial undamaged elastic stiffness tensor. It is important to note that the plastic behavior and creep behavior are formulated in the effective (undamaged) stress space, and, therefore, the evolution of the plastic strain and creep strain should be controlled by the effective stress rather than the nominal stress. Furthermore, considering that the degradation of stiffness in tension may differ from that in compression, the biscalar damage scheme is adopted for which the damage tensor is split into two components

$$\mathbb{D} = d^+\mathbb{P}^+ + d^-\mathbb{P}^- \tag{6}$$

where the scalar variables d^+ and d^- represent the tensile and the compressive damage variables; $\mathbb{P}^+$ and $\mathbb{P}^-$ = fourth-order projection tensors. The derivation of Eq. (6) is provided in Appendix I. Based on the framework of damage plasticity theory, numerous equations of damage evolution and plasticity evolution have been proposed. In the present paper, the damage evolution proposed by Wu et al. (2006) and the phenomenological plasticity evolution proposed by Ren et al. (2015) are adopted (see Appendix I for a detailed discussion).

In summary, the constitutive equation of the coupled creep-damage-plasticity model for concrete could be expressed as

$$\boldsymbol{\sigma} = (\mathbb{I} - \mathbb{D}):\mathbb{E}_0:(\boldsymbol{\varepsilon} - \boldsymbol{\varepsilon}^p - \boldsymbol{\varepsilon}^c) \tag{7}$$

Summarizing, for low stress levels, the concrete stress is relatively small, and concrete is not significantly damaged; Eq. (5) is thus simplified to an elastic-plastic-creep model. In the time scale of typical short-term loading conditions, there is not enough time to develop creep, and it reduces to a classical damage plasticity model. However, for long-term loading at moderate and high stress levels, the concrete response is associated with significant and simultaneous damage growth, plastic deformation, and creep behavior.

Creep Modeling

Many theoretical and empirical models have been proposed to characterize creep phenomena. The most widely used theoretical models rely on the generalized Maxwell or Kelvin models (Bažant and Chern 1985; Bažant and Prasannan 1989; Bažant and Planas 1997), wherein a number of springs and dashpots are assembled in parallel or series. The empirical models, such as the ACI 209R-92 model (ACI 2008), the B3 model (Bažant and Murphy 1995; Bažant and Baweja 2000), the GL 2000 model (Gardner and Zhao 1993; Gardner 2000; Gardner and Lockman 2001) and the *fib* MC 2010 model (*fib* 2010), are most often optimal curve fittings of available

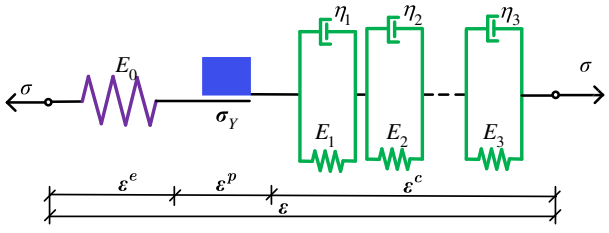

Fig. 1. Schematic representation of strain additivity assumption.

J. Eng. Mech., 2020, 146(5): 04020027

Downloaded from ascelibrary.org by University of Houston on 08/11/20. Copyright ASCE. For personal use only; all rights reserved.

experimental data. Most of these models are adopted in design recommendations and are widely used in practice.

Linear Creep Model

In the present paper, the ACI model (ACI 209R-92) is chosen to calculate the creep strain under uniaxial stress states because it is widely applied and well accepted by designers and researchers for engineering applications. This model is primarily suitable for the linear creep range that is typical of most civil engineering-related structures. For completeness, the ACI model is summarized in Appendix II. Given the elastic strain, $\boldsymbol{\varepsilon}^e$, the ACI model is generalized to multiaxial stress states as follows:

$$\boldsymbol{\varepsilon}^c(t,t_0) = \varphi(t,t_0)\boldsymbol{\varepsilon}^e = \frac{(t-t_0)^a}{b+(t-t_0)^a}\varphi_\infty \boldsymbol{\varepsilon}^e \tag{8}$$

Eq. (8) shows that the creep strain is proportional to the elastic strain. By differentiating Eq. (8) with respect to time, the creep strain rate is obtained

$$\dot{\boldsymbol{\varepsilon}}^c(t,t_0) = \dot{\varphi}(t,t_0)\boldsymbol{\varepsilon}^e + \varphi(t,t_0)\dot{\boldsymbol{\varepsilon}}^e \tag{9}$$

The first term on the right-hand side of Eq. (9) is related to the change of creep coefficient, and the second one represents the contribution of the change in time of the elastic strain.

If the initial loading stage is relatively short and the load level is maintained constant in time, the change of the elastic strain is negligible so that the second term in Eq. (9) can be omitted, and the computational effort is significantly reduced. For such cases

$$\dot{\boldsymbol{\varepsilon}}^c(t,t_0) \approx \dot{\varphi}(t,t_0)\boldsymbol{\varepsilon}^e \tag{10}$$

Similar to the damage and the plasticity, the creep evolution under tensile and compressive stress states is allowed to differ. Thus, the creep strain rate is decomposed as follows:

$$\dot{\boldsymbol{\varepsilon}}^c(t,t_0) = \dot{\boldsymbol{\varepsilon}}^{c+}(t,t_0) + \dot{\boldsymbol{\varepsilon}}^{c-}(t,t_0) \tag{11}$$

where the tensile creep strain rate, $\dot{\boldsymbol{\varepsilon}}^{c+}(t,t_0)$, and the compressive creep strain rate, $\dot{\boldsymbol{\varepsilon}}^{c-}(t,t_0)$, are in turn written as

$$\begin{aligned}\dot{\boldsymbol{\varepsilon}}^{c+}(t,t_0) &\approx \dot{\varphi}^+(t,t_0)\boldsymbol{\varepsilon}^{e+} = \dot{\varphi}^+(t,t_0)\mathbb{E}_0^{-1}{:}\bar{\boldsymbol{\sigma}}^+\\ \dot{\boldsymbol{\varepsilon}}^{c-}(t,t_0) &\approx \dot{\varphi}^-(t,t_0)\boldsymbol{\varepsilon}^{e-} = \dot{\varphi}^-(t,t_0)\mathbb{E}_0^{-1}{:}\bar{\boldsymbol{\sigma}}^-\end{aligned} \tag{12}$$

In the present model, the effective stress is adopted to calculate creep strain. In addition, due to a lack of sufficient experimental data, it is assumed that the same evolution law is adopted to describe creep strain development under tensile and compressive stress states in the illustrative examples presented in the "Numerical Examples" section.

Nonlinear Creep Model

For medium and high stress levels, the dependence of creep strain on stress becomes nonlinear and is accounted for through a damage-dependent influence function. The functions $h^\pm(\cdot)$ are defined in terms of corresponding damage variables

$$h^\pm(d^\pm) = 1 + c_1^\pm (d^\pm)^{c_2^\pm} \tag{13}$$

where two empirical parameters $c_1^\pm$ and $c_2^\pm$ reflect the effects of concrete damage, especially at medium and high stress levels, on the creep strain. This is a simplified expression of the nonlinear dependence of creep on stress. The specific values of $c_1^\pm$ and $c_2^\pm$ need to be calibrated from the experimental data, and in the following representative numerical examples $c_1^\pm = 9$, $c_2^\pm = 0.91$ are adopted. The evolution of nonlinear creep strain is obtained by multiplying Eq. (12) by Eq. (13)

$$\begin{aligned}\dot{\boldsymbol{\varepsilon}}^{c+}(t,t_0) &\approx h^+\dot{\varphi}^+(t,t_0)\boldsymbol{\varepsilon}^{e+} = h^+\dot{\varphi}^+(t,t_0)\mathbb{E}_0^{-1}{:}\bar{\boldsymbol{\sigma}}^+\\ \dot{\boldsymbol{\varepsilon}}^{c-}(t,t_0) &\approx h^-\dot{\varphi}^-(t,t_0)\boldsymbol{\varepsilon}^{e-} = h^-\dot{\varphi}^-(t,t_0)\mathbb{E}_0^{-1}{:}\bar{\boldsymbol{\sigma}}^-\end{aligned} \tag{14}$$

The evolution of each creep strain component is governed by the corresponding damage variable, temporal variables, and the effective stress which is directly related to the elastic strain. The function $h^\pm(\cdot)$ indicates that the evolution of damage is a prerequisite for the evolution of nonlinear creep. For relatively low stress levels, negligible damage occurs during the whole loading process. In such cases, the damage-dependent influence function $h^\pm(\cdot)$ is nearly equal to one, and, therefore, the nonlinear creep evolution reduces to a linear creep evolution. Increasing the stress level, damage begins to growth and develop. Through the function $h^\pm(\cdot)$, a significant nonlinear amplification of creep strain caused by damage can be reflected. Thus, the coupling between damage and creep strain is considered in a phenomenological reduced form.

As stated previously, the present nonlinear creep model is suitable to describe linear creep behavior under low stress levels and nonlinear creep behavior under medium and high stress levels, but not apply to extremely high stress levels. This is not a serious limitation for most civil engineering applications, considering that they are not typically loaded by extremely high stresses that trigger tertiary creep.

Creep Strain Algorithm

To calculate the creep strain according to the present theory, the following three conditions need to be fulfilled:

1. The external load is constant during loading, i.e., $\dot{\boldsymbol{\sigma}} \approx 0$;
2. The ratio of the loading application time to the duration of loading is very small. Assuming t_1 indicates that loading is complete and the load begins to remain unchanged, $(t_1 - t_0) \ll (t - t_1)$; and
3. The stress levels experienced by structural components must be below approximately 70% of the concrete strength to ensure the absence of tertiary creep.

In view of the above conditions, an explicit numerical scheme is developed to integrate creep strain. Adopting the backward Euler method and Eq. (14), the creep strain increment could be calculated using Eq. (15)

$$\Delta\boldsymbol{\varepsilon}^c(t,t_0) = \Delta\boldsymbol{\varepsilon}^{c+}(t,t_0) + \Delta\boldsymbol{\varepsilon}^{c-}(t,t_0) \tag{15}$$

where the tensile creep strain increment, $\Delta\boldsymbol{\varepsilon}^{c+}(t,t_0)$, and the compressive creep strain increment, $\Delta\boldsymbol{\varepsilon}^{c-}(t,t_0)$, are expressed by

$$\begin{aligned}\Delta\boldsymbol{\varepsilon}^{c+}(t,t_0) &= h^+(d_{n+1}^+)\Delta\varphi_{n+1}^+(t,t_0)\mathbb{E}_0^{-1}{:}\bar{\boldsymbol{\sigma}}_{n+1}^+\\ \Delta\boldsymbol{\varepsilon}^{c-}(t,t_0) &= h^-(d_{n+1}^-)\Delta\varphi_{n+1}^-(t,t_0)\mathbb{E}_0^{-1}{:}\bar{\boldsymbol{\sigma}}_{n+1}^-\end{aligned} \tag{16}$$

Thus, the creep strain at time step $n+1$ is given by

$$\boldsymbol{\varepsilon}_{n+1}^c(t,t_0) = \boldsymbol{\varepsilon}_n^c(t,t_0) + \Delta\boldsymbol{\varepsilon}^{c+}(t,t_0) + \Delta\boldsymbol{\varepsilon}^{c-}(t,t_0) \tag{17}$$

From the viewpoint of numerical algorithms, it is more convenient to use creep stress than creep strain. Therefore, the following representation of creep stress is adopted in the computations

Downloaded from ascelibrary.org by University of Houston on 08/11/20. Copyright ASCE. For personal use only; all rights reserved.

$$\dot{\sigma}^{c+}(t,t_0) = h^+(d^+)\dot{\varphi}^+(t,t_0)\bar{\boldsymbol{\sigma}}^+$$
$$\dot{\sigma}^{c-}(t,t_0) = h^-(d^-)\dot{\varphi}^-(t,t_0)\bar{\boldsymbol{\sigma}}^- \quad (18)$$

In the proposed nonlinear creep model, five creep-related parameters are empirical and are of two kinds; $\varphi_\infty^\pm$, $a^\pm$, $b^\pm$ are free and must be fitted using the results of long-term experiment tests, whereas $c_1^\pm$, $c_2^\pm$ remain approximately constant for practical applications.

Numerical Scheme

In view of the previously described nonlinear creep theory, the creep strain term is introduced into the damage-plasticity model proposed by Wu et al. (2006) and Ren et al. (2015) to consider the coupled creep, damage, and plasticity effects. The constitutive law of the coupled creep-damage-plasticity model is summarized as follows:

$$\boldsymbol{\sigma} = (1-d^+)\mathbb{E}_0{:}(\boldsymbol{\varepsilon}^+ - \boldsymbol{\varepsilon}^{p+} - \boldsymbol{\varepsilon}^{c+}) + (1-d^-)\mathbb{E}_0{:}(\boldsymbol{\varepsilon}^- - \boldsymbol{\varepsilon}^{p-} - \boldsymbol{\varepsilon}^{c-}) \quad (19)$$

According to the concept of operator splitting (Ju 1989; Simo and Hughes 2006), the computation of the instantaneous stress from the instantaneous strain could be decomposed into three parts; elastic, plastic, and damage. Considering that the proposed model is applicable for the sustained load situation, the creep part is added to the algorithm. Thus, the numerical algorithm that we adopted consists of four parts; the elastic-predictor, plastic-corrector, damage-corrector, and creep-calculation steps.

In the computational analysis procedure, it is assumed that the calculation at previous time step k has been completed (All the state variables and internal variables at time step k are known). By prescribing an increment in total strain, the aim of the proposed algorithm is to update all the state variables and internal variables to the next time step (k + 1).

In the elastic-predictor step, the evolutions of plasticity, creep and damage are frozen. The trial state of the effective stress is first computed as follows:

$$\bar{\boldsymbol{\sigma}}_{k+1}^{trial} = \mathbb{E}_0{:}\boldsymbol{\varepsilon}_{k+1} - \sigma_k^p - \sigma_k^c \quad (20)$$

The trial effective stress is split into positive and negative components using the spectral decomposition method. Subsequently, the trial states of the damage release rates, $(Y^\pm)_{k+1}^{trial}$, and the energy equivalent strains, $(\varepsilon_{eq}^{e\pm})_{k+1}^{trial}$, could be explicitly obtained. Two situations including tensile and compressive states are discussed in detail next. According to the trial solutions, the damage criteria are adopted to judge whether or not damage evolves

$$(R^\pm)_{k+1}^{trial} = |(\varepsilon_{eq}^{e\pm})_{k+1}^{trial}| - |(r_e^\pm)_k| \le 0 \quad (21)$$

If Eq. (21) is satisfied, the current time step remains elastic. Neither plastic strain nor damage variables evolve because the damage variables govern the evolution of the damage and plasticity. Then, the updated variables at time step k + 1 are equal to ones at time step k

$$\boldsymbol{\varepsilon}_{k+1}^{p\pm} = \boldsymbol{\varepsilon}_k^{p\pm}, \quad d_{k+1}^\pm = d_k^\pm, \quad (r_e^\pm)_{k+1} = (r_e^\pm)_k \quad (22)$$

On the other hand, if Eq. (21) is not satisfied in the elastic-predictor step, plastic strain and damage variables evolve between time step k and time step k + 1, and the analysis goes into the corrector step.

In the damage-corrector step, the damage thresholds, $r_e^\pm$, are updated

$$(r_e^+)_{k+1} = \max\{\varepsilon_{eq}^{e+}, (r_e^+)_k\}$$
$$(r_e^-)_{k+1} = \max\{\varepsilon_{eq}^{e-}, (r_e^-)_k\} \quad (23)$$

and the damage variables are

$$d_{k+1}^+ = g^+[(r_e^+)_{k+1}]$$
$$d_{k+1}^- = g^-[(r_e^-)_{k+1}] \quad (24)$$

In the plastic-corrector step, the computation of the plastic strain increment is explicitly determined as a function of the damage variable and the effective stress increment. The tensile and compressive plastic stress increments are computed as follows:

$$\Delta\boldsymbol{\sigma}^{p+} = H(d_{k+1}^+ - d_k^+)\xi_p^+(d_{k+1}^+)^{n_p^+}[\bar{\boldsymbol{\sigma}}_{k+1}^+ - \bar{\boldsymbol{\sigma}}_k^+] \approx H(d_{k+1}^+ - d_k^+)\xi_p^+(d_{k+1}^+)^{n_p^+}[(\bar{\boldsymbol{\sigma}}^+)_{k+1}^{trial} - \bar{\boldsymbol{\sigma}}_k^+]$$
$$\Delta\boldsymbol{\sigma}^{p-} = H(d_{k+1}^- - d_k^-)\xi_p^+(d_{k+1}^-)^{n_p^-}[\bar{\boldsymbol{\sigma}}_{k+1}^- - \bar{\boldsymbol{\sigma}}_k^-] \approx H(d_{k+1}^- - d_k^-)\xi_p^+(d_{k+1}^-)^{n_p^-}[(\bar{\boldsymbol{\sigma}}^-)_{k+1}^{trial} - \bar{\boldsymbol{\sigma}}_k^-] \quad (25)$$

The trial effective stress components, $(\bar{\boldsymbol{\sigma}}^\pm)_{k+1}^{trial}$, are adopted to replace the real effective stress components, $(\bar{\boldsymbol{\sigma}}^\pm)_{k+1}$. This approach not only is able to avoid complex and time-consuming iterations but also has been proven to yield good results for concrete structures, as demonstrated by extensive comparisons with test data in Ren et al. (2015).

The creep strain at time step k + 1 is computed in the creep-calculation step, which needs to consider the effects of time. According to the relationships defined in section "Creep Modeling," the creep strain increment is explicitly determined as a function of current time, damage variables, and the effective stress using Eq. (16). Then, the creep stress components under tensile and compressive stress states are computed by

$$\boldsymbol{\sigma}_{k+1}^{c+} = \boldsymbol{\sigma}_k^{c+} + \Delta\boldsymbol{\sigma}^{c+} = \boldsymbol{\sigma}_k^{c+} + h^+(d_{n+1}^+)\Delta\varphi_{n+1}^+(t,t_0)[\bar{\boldsymbol{\sigma}}^+]_{k+1}^{trial}$$
$$\boldsymbol{\sigma}_{k+1}^{c-} = \boldsymbol{\sigma}_k^{c-} + \Delta\boldsymbol{\sigma}^{c-} = \boldsymbol{\sigma}_k^{c-} + h^-(d_{n+1}^-)\Delta\varphi_{n+1}^-(t,t_0)[\bar{\boldsymbol{\sigma}}^-]_{k+1}^{trial} \quad (26)$$

Similar to the simplified method in the plastic-corrector step, the trial effective stress components, $(\bar{\boldsymbol{\sigma}}^\pm)_{k+1}^{\text{trial}}$, are adopted to replace the effective stress components, $(\bar{\boldsymbol{\sigma}}^\pm)_{k+1}$, in the creep-calculation step.

Finally, the effective stress components at time step k + 1 are updated by the following relationships

$$\bar{\boldsymbol{\sigma}}_{k+1}^+ = \mathbb{E}_0{:}\boldsymbol{\varepsilon}_{k+1}^+ - \boldsymbol{\sigma}_{k+1}^{p+} - \boldsymbol{\sigma}_{k+1}^{c+}$$
$$\bar{\boldsymbol{\sigma}}_{k+1}^- = \mathbb{E}_0{:}\boldsymbol{\varepsilon}_{k+1}^- - \boldsymbol{\sigma}_{k+1}^{p-} - \boldsymbol{\sigma}_{k+1}^{c-} \quad (27)$$

Then, the stress at time step $k+1$ could be expressed as follows:

$$\boldsymbol{\sigma}_{k+1} = (1-d_{k+1}^+)\bar{\boldsymbol{\sigma}}_{k+1}^+ + (1-d_{k+1}^-)\bar{\boldsymbol{\sigma}}_{k+1}^- \quad (28)$$

At this stage of the computational procedure, all the state variables and the internal variables at time step k + 1 are updated. The plastic-corrector step and creep-calculation step are used primarily

Downloaded from ascelibrary.org by University of Houston on 08/11/20. Copyright ASCE. For personal use only; all rights reserved.

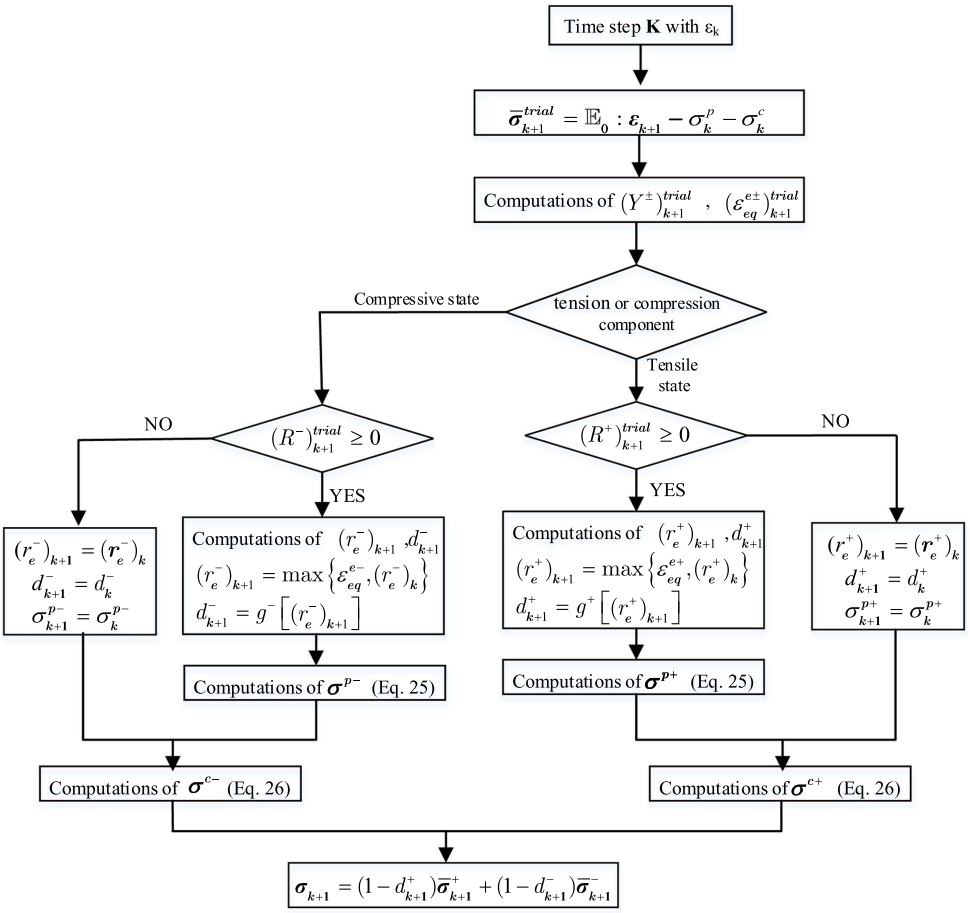

Fig. 2. Explicit numerical algorithm.

for updating the effective stress, whereas the damage corrector step is used to describe the reduction effect of damage variables on the effective stress. The total numerical implementation is straightforward. All involved numerical analyses could be directly calculated without an iterative process, which greatly improves the computational efficiency.

Furthermore, according to the work of Ren et al. (2015), the proposed numerical scheme at the material level is unconditionally stable; the numerical stability of the model is governed at the structural level. During numerical simulation, adopting a small-time incremental step guarantees the stability of explicit methods. For additional details and discussion related to the stability and convergence of the proposed numerical algorithm, the reader is referred to Ren et al. (2015).

The whole explicit numerical algorithm for the coupled creep-damage-plasticity model is summarized in Fig. 2.

Table 1. Model parameters for uniaxial compression tests

Item	Value
Elasticity	$E_0(21500\ \text{MPa}), \upsilon(0.2)$
Compressive strength	$f_c(47.5\ \text{MPa})$
Damage	$\alpha_c(0.5)$
Plasticity	$\xi_p^-(0.4), n_p^-(0.1)$
Creep	$\varphi_\infty^-(5.4)$
	$a^-(14), b^-(0.6)$
	$c_1^-(9), c_2^-(0.91)$

Numerical Examples

The coupled creep-damage-plasticity model proposed in the present study was implemented in the finite-element (FE) software ABAQUS version 6.13 through the user-defined material model feature for the simulation of concrete behavior under long-term

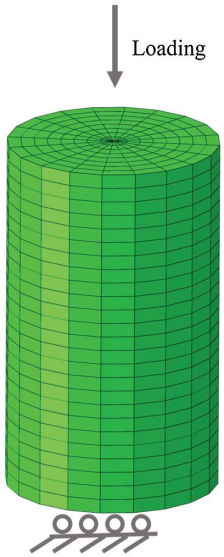

Fig. 3. Representative finite-element mesh of uniaxial tests.

Downloaded from ascelibrary.org by University of Houston on 08/11/20. Copyright ASCE. For personal use only; all rights reserved.

loading condition. The illustrative examples presented in this paper are two-dimensional analysis because their purpose is to illustrate the predictions of the present constitutive model.

Uniaxial Tests

The first verification exercise involves the experimental results from a series of plain concrete cylinder tests under uniaxial sustained stress (Freudenthal and Roll 1958; Roll 1964). The cylinder specimens at the age of 28 days were subjected to a sustained compressive stress in the range of 20%–65% of the compressive strength, f_c. Relevant model parameters are listed in Table 1. It is noteworthy that these model parameters remain unchanged in the numerical simulations of all the uniaxial tests, and the values in brackets are chosen for simulations. Considering the axisymmetric characteristics of the cylinder, the axisymmetric solid element, CAX4R, is used to model concrete. A representative FE mesh is shown in Fig. 3.

Fig. 4 compares the experimental results at different sustained stress levels with those obtained from numerical simulations. It is observed that both linear creep behavior and nonlinear creep behavior are well predicted. Comparison of the numerical results using the linear creep model and the nonlinear creep model is shown in Fig. 5. As expected, at low (high) stress levels, the simulated results using the linear creep model coincide (do not coincide) with those of the nonlinear creep model. Generally, the predictions using the proposed nonlinear creep model agree reasonably well with the experimental results both for low and high stress levels.

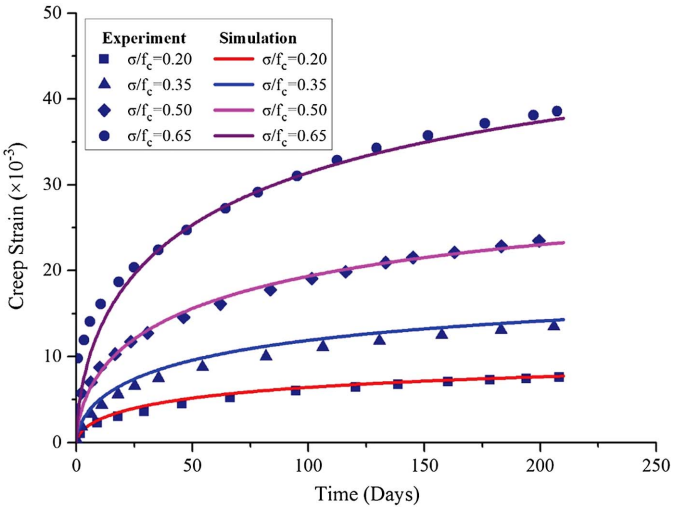

Fig. 4. Simulation of creep tests at different stress levels: Comparison of results using the proposed nonlinear creep model and experiment.

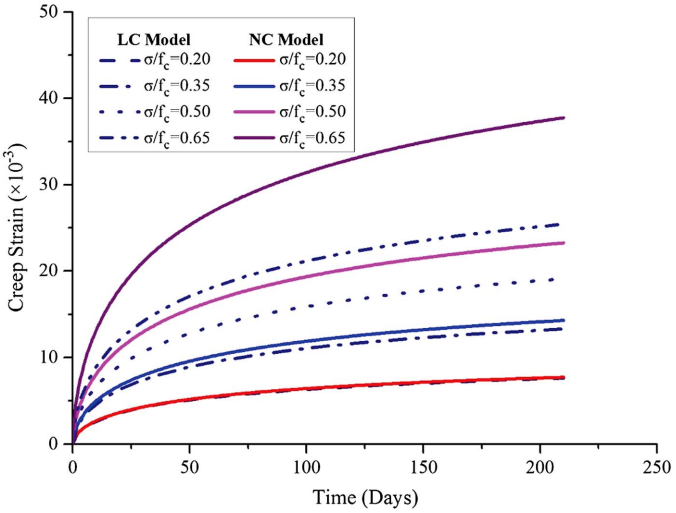

Fig. 5. Comparison of numerical results at different stress levels using linear creep model (LC Model) and nonlinear creep model (NC Model).

Creep Tests of Simply Supported RC Beam

A plain concrete prism specimen and two simply supported RC beams performed by Clarke (1987) are simulated. The simulation of the prism specimen is designed to calibrate the creep-related parameters, with which the long-term deformations of RC beams are predicted. These three tests use the same batch of concrete and are exposed to the same environment.

The prism, $100 \times 100 \times 200$ mm, was subjected to a sustained compressive stress of 10 MPa at the age of 28 days. Two beams without stirrups were loaded at the three points of the span. The beam geometry is shown in Fig. 6, and the beam specimen dimensions and loading program are listed in Table 2.

In the simulation, four-node plane stress elements are used to model the concrete, and two-node truss elements are used to model the reinforcing bar. The steel bars are modeled as elastic-perfectly

Table 2. Experiment program for RC beam

Parameter	Unit	Specimen number	
		A2	B1
Specimen size	a/mm	700	700
	z/mm	700	700
	b/mm	100	100
	h/mm	152	152
	h_0/mm	130	130
Shear span ratio	λ	5.38	5.38
Reinforcement area	A_s/mm^2	157.1(0+2D10)	314.2(2D10+2D10)
Compressive strength	f_c/MPa	32.4	32.4
Load	P/KN	10	10

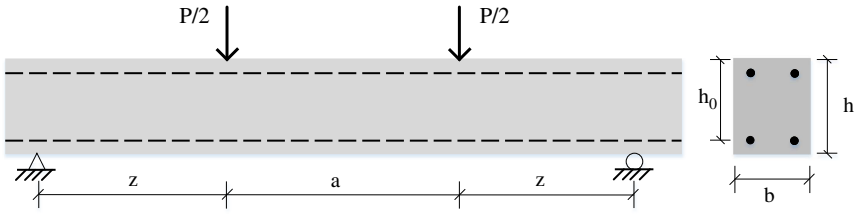

Fig. 6. Geometry of the simply supported beam.

Downloaded from ascelibrary.org by University of Houston on 08/11/20. Copyright ASCE. For personal use only; all rights reserved.

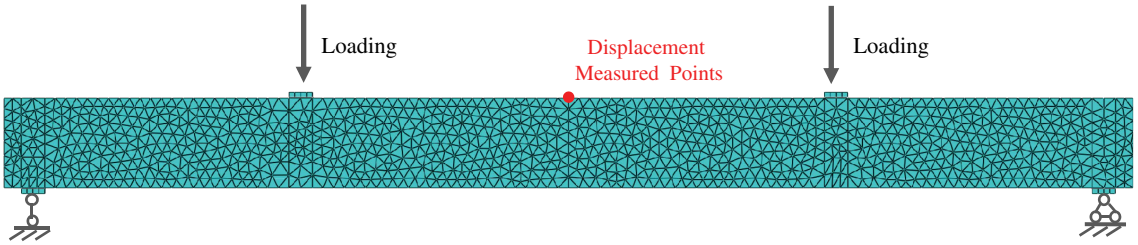

Fig. 7. Representative finite-element mesh of RC beam.

Table 3. Model parameters for RC beam

Parameter	Series I
Elasticity	$E_0(22000\ \text{MPa}), \upsilon(0.2)$
Damage	$\alpha_t(0.1), \alpha_c(0.1)$
Plasticity	$\xi_p^+(0), n_p^+(0.1)$
	$\xi_p^-(0.4), n_p^-(0.1)$
Creep	$\varphi_\infty^\pm(2.93)$
	$a^\pm(13), b^\pm(0.6)$
	$c_1^\pm(9), c_2^\pm(0.91)$

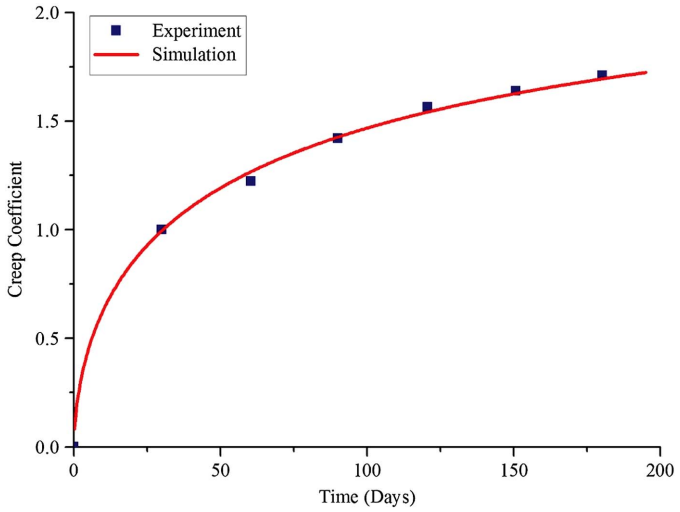

Fig. 8. Calibration of the prism specimen: Comparison of results given by the proposed model and experiment.

plastic with material parameters: $E_s = 200$ GPa, $f_y = 345$ MPa. It is assumed that there is no bond-slip between concrete and steel. A representative FE mesh is shown in Fig. 7.

The creep-related parameters calibrated by the prism test are listed in Table 3. The simulated creep coefficient, defined as the ratio of the creep deformation to the initial deformation, is compared with the experiment in Fig. 8. And Fig. 9 shows the comparison of the prediction results and experimental data obtained from the RC beams. The simulated evolution of specimen A2 agrees very well with the experiment at all time, whereas some differences are observed for specimen B1, which are attributed to the random nature of concrete properties. Contours of simulated beam tensile damage are shown in Fig. 10 and are typical of those reflected by experimental observations. Because the level of sustained load is low, both RC beams exhibit modest levels of tensile damage. These calibration-prediction examples illustrate the strong applicability and good prediction capability of the proposed model.

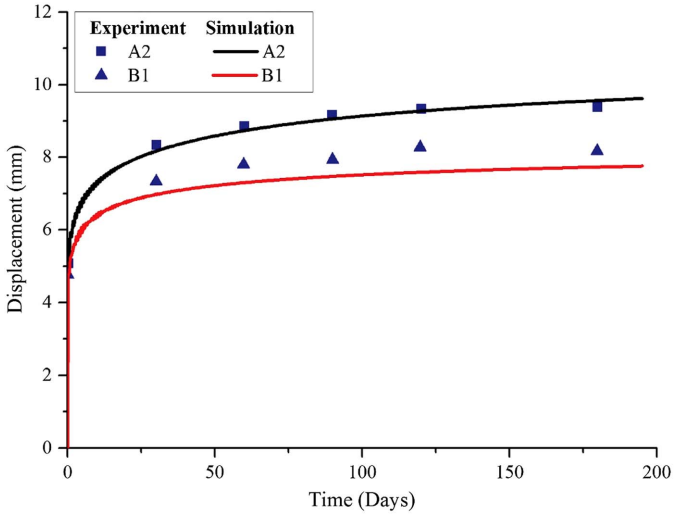

Fig. 9. Predictions of the RC beams: Comparison of results given by the proposed model and experiment.

Creep Tests of RC Short Column

This section presents numerical simulations of the experiments performed on reinforced high strength concrete short columns by Geng et al. (2013) whose geometry is shown in Fig. 11. At the age of 28 days, the columns are subjected to a uniform pressure along their length. Two specimens with different reinforcement ratio are simulated with the specific loading program listed in Table 4. Related concrete material parameters are listed in Table 5. The steel reinforcement material parameters are: $E_s = 200$ GPa, $f_y = 345$ MPa. The simulation procedure is the same as the one used in the preceding RC beam simulations, and the illustrative FE mesh is shown in Fig. 12.

The evolution of the creep coefficient is simulated and compared with the experimental data in Fig. 13. Relatively good agreement is observed for both specimens. There is a modest discrepancy between the numerical results and experimental results, particularly in the final stage of specimen RCC1 and the initial stage of specimen RCC2, which can be attributed to the inability of the simplified representation of the complex test environment. The results suggest that the model offers promise for capturing creep response under compressive loading.

Fig. 14 shows the simulations of the RC short column for four stress levels; 20%, 35%, 50%, and 65% of compressive strength, using the linear creep model and nonlinear creep model. As expected, an increasing the stress level produces an increasing difference between the results of the linear creep model and those of the nonlinear creep model. It is also noted that larger creep strain values are obtained using the nonlinear creep model.

Downloaded from ascelibrary.org by University of Houston on 08/11/20. Copyright ASCE. For personal use only; all rights reserved.

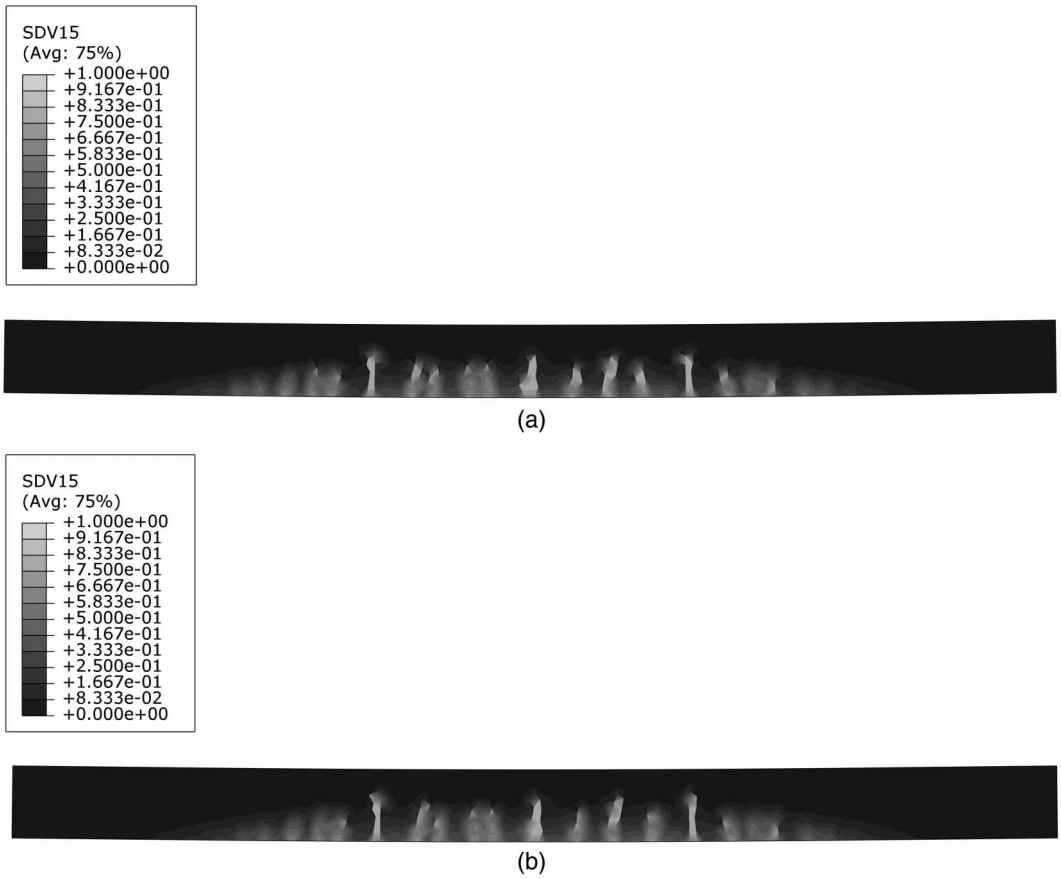

Fig. 10. Simulation tensile damage contours of two simply supported RC beam: (a) specimen A2; and (b) specimen B1.

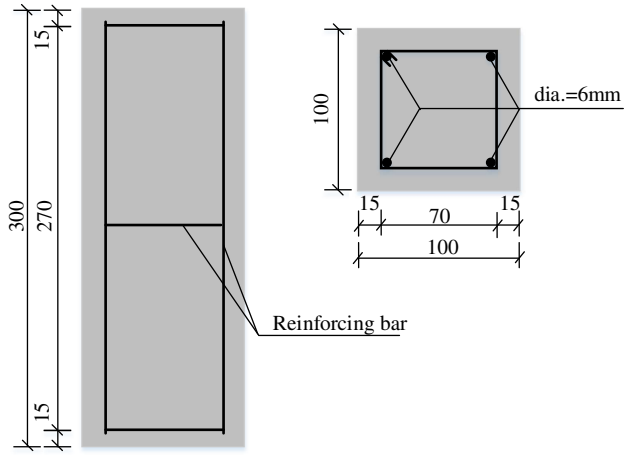

Fig. 11. Geometry of RC short column.

Table 4. Experiment program for RC column

Parameter	Unit	Specimen number	
		RCC1	RCC2
Sectional area	A/mm^2	10,000	10,000
Reinforcement area	A_s/mm^2	0	113.1(2D6+2D6)
Reinforcement ratio	ρ	0%	1.1%
Load	P/KN	250	250
Stress	σ/MPa	25	25
Stress level	σ/f_c	39%	39%

Table 5. Model parameters for RC column

Item	Value
Elasticity	$E_0(41{,}700\ \text{MPa}), v(0.2)$
Compressive strength	$f_c(64.5\ \text{MPa})$
Damage	$\alpha_t(0.1), \alpha_c(0.1)$
Plasticity	$\xi_p^+(0), n_p^+(0.1)$
	$\xi_p^-(0.4), n_p^-(0.1)$
Creep	$\varphi_\infty^\pm(0.94)$
	$a^\pm(13), b^\pm(0.6)$
	$c_1^\pm(9), c_2^\pm(0.91)$

The effect of the reinforcement ratio on creep behavior has also been investigated. For this purpose, the simulations of the RC short column with four different reinforcement ratios, 0%, 0.5%, 1.1%, and 3.0%, are performed. The numerical results are depicted in Fig. 15. The results show that an increase in reinforcement ratio leads to the reduction in creep deformation.

Conclusion

A coupled creep-damage-plasticity model for concrete under long-term loading condition has been proposed which takes into account linear and nonlinear creep behavior. The main conclusions are as follows:

1. A model that combines the continuum damage theory and the phenomenological plasticity model proposed by Ren et al. (2015)

J. Eng. Mech., 2020, 146(5): 04020027

Downloaded from ascelibrary.org by University of Houston on 08/11/20. Copyright ASCE. For personal use only; all rights reserved.

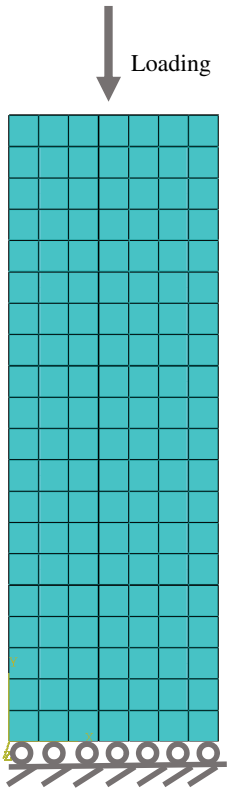

Fig. 12. Representative finite-element mesh of RC column.

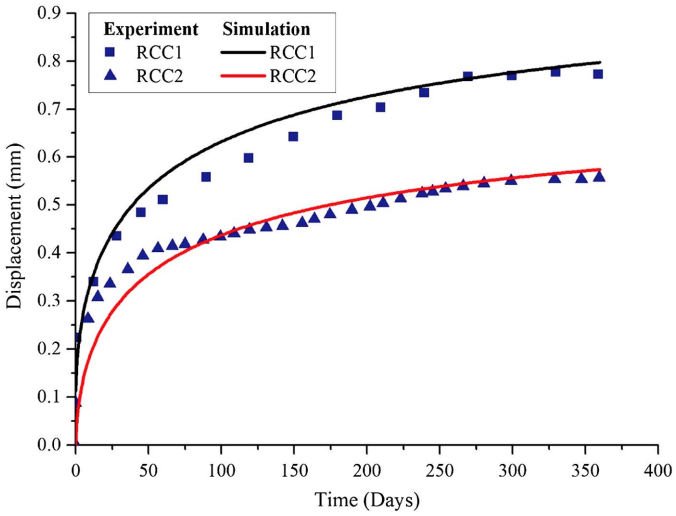

Fig. 13. Simulation of reinforcement high-strength concrete short column test: Comparison of results given by the proposed model and experiment.

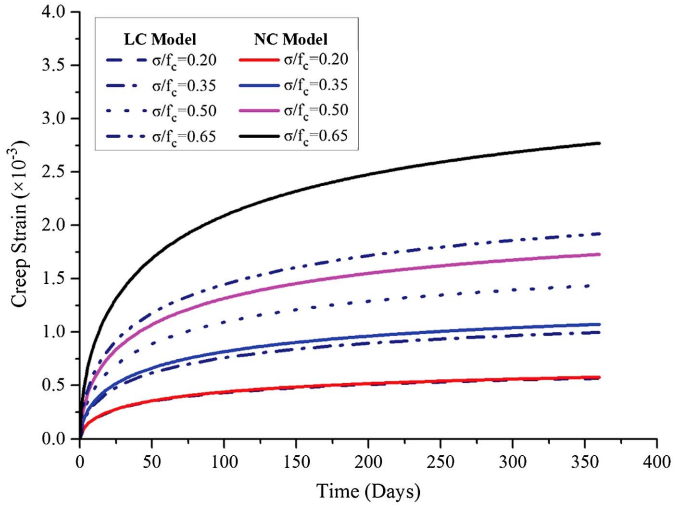

Fig. 14. Simulation of RC short column test with different stress levels using linear creep model (LC Model) and nonlinear creep model (NC Model).

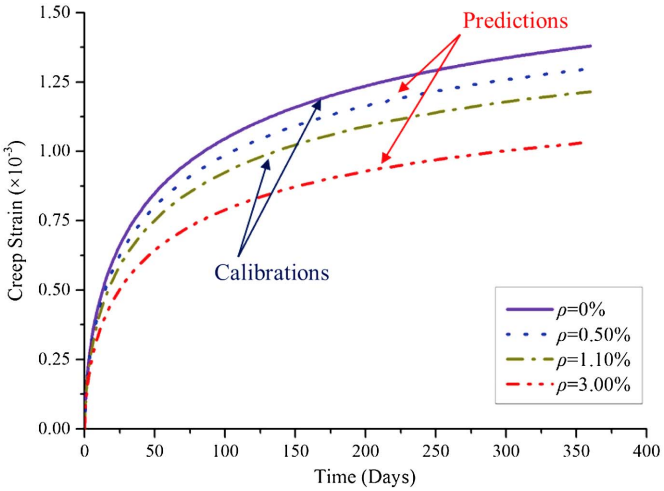

Fig. 15. Simulation of RC short column test with different reinforcement ratio ρ.

offers a basic framework for characterizing the constitutive behavior of concrete. The advantage of the proposed model lies in its ability to simultaneously capture stiffness degradation and residual deformation.

2. Based on the assumption of strain additivity, a damage-plasticity model is extended to account for the creep effect by adding the creep strain to the damage-plasticity model using a modified version of the widely-adopted and used ACI linear creep model.
3. For medium and high stress levels, nonlinear creep is introduced by multiplying the current creep strain by a damage-dependent influence function. This function reflects the coupling relationship between damage and creep.
4. Using the operator splitting method, an explicit algorithm has been developed for the numerical implementation of the proposed model. This algorithm does not require an iterative process, which greatly improves the computation efficiency.
5. The illustrative examples of the monolithic concrete subjected to uniaxial compression, and reinforced concrete beams subjected flexural loads, and reinforced concrete columns subjected to compression, suggest that the proposed constitutive model and computational algorithms can capture the behavior of concrete structures under long-term loading.
6. Several numerical examples are performed whose results are consistent with the experimental results. These illustrative simulations suggest that the proposed coupled creep-damage-plasticity model could account for the long-term behavior of

Downloaded from ascelibrary.org by University of Houston on 08/11/20. Copyright ASCE. For personal use only; all rights reserved.

concrete and can therefore be applied to practical engineering design problems.

Appendix I. Damage-Plasticity Model

The damage plasticity model proposed by Wu et al. (2006) and Ren et al. (2015) is summarized. The constitutive law is expressed as

$$\boldsymbol{\sigma} = (\mathbb{I} - \mathbb{D}):\bar{\boldsymbol{\sigma}} = (\mathbb{I} - \mathbb{D}):\mathbb{E}_0:(\boldsymbol{\varepsilon} - \boldsymbol{\varepsilon}^p) \tag{29}$$

Considering the different behaviors in tension and in compression, the stress tensor (nominal or effective) is decomposed into positive (tensile) and negative (compressive) components as follows:

$$\boldsymbol{\sigma} = \boldsymbol{\sigma}^+ + \boldsymbol{\sigma}^-, \qquad \bar{\boldsymbol{\sigma}} = \bar{\boldsymbol{\sigma}}^+ + \bar{\boldsymbol{\sigma}}^- \tag{30}$$

Based on the spectral decomposition method (Simo and Ju 1987a, b; Voyiadjis and Abu-Lebdeh 1994; Voyiadjis et al. 2008), the tensile effective stress and the compressive effective stress are expressed as

$$\begin{aligned} \bar{\boldsymbol{\sigma}}^+ &= \mathbb{P}^+:\bar{\boldsymbol{\sigma}} \\ \bar{\boldsymbol{\sigma}}^- &= \bar{\sigma} - \bar{\boldsymbol{\sigma}}^+ = \mathbb{P}^-:\bar{\boldsymbol{\sigma}} \end{aligned} \tag{31}$$

And the fourth-order projection tensors read

$$\begin{aligned} \mathbb{P}^+ &= \sum_i \boldsymbol{H}(\hat{\bar{\boldsymbol{\sigma}}}_i)\boldsymbol{p}^{(i)} \otimes \boldsymbol{p}^{(i)} \otimes \boldsymbol{p}^{(i)} \otimes \boldsymbol{p}^{(i)} \\ \mathbb{P}^- &= \mathbb{I} - \mathbb{P}^+ \end{aligned} \tag{32}$$

where $\hat{\bar{\boldsymbol{\sigma}}}_i$ and $\boldsymbol{p}^{(i)}$ are the i-th eigenvalue and eigenvector of the effective stress tensor, and $H(\cdot)$ is the Heaviside step function, defined as

$$H(x) = \begin{cases} 0 & x < 0 \\ 1 & x \geq 0 \end{cases} \tag{33}$$

Based on the decomposition of the stress, one can assume that Eq. (3) is valid for the tensile and compressive components of the stress

$$\begin{aligned} \boldsymbol{\sigma}^+ &= (1 - d^+)\bar{\boldsymbol{\sigma}}^+ \\ \boldsymbol{\sigma}^- &= (1 - d^-)\bar{\boldsymbol{\sigma}}^- \end{aligned} \tag{34}$$

Substituting Eqs. (31) and (34) into Eq. (30), the explicit expression of the fourth-order damage tensor can be obtained as follows

$$\mathbb{D} = d^+\mathbb{P}^+ + d^-\mathbb{P}^- \tag{35}$$

This type of the damage tensor is referred to as the biscalar damage scheme.

Damage Evolution

Based the theory of irreversible thermodynamics, the energy conjugate quantities of the tensile and the compressive damages, which are defined as the damage release rates, are used as the driving forces of the damage evolution

$$Y^\pm = -\frac{\partial \psi}{\partial d^\pm} \tag{36}$$

where the superscripts "±" denotes "+" and "−", which represent tensile and compressive components, respectively; ψ = Helmholtz free energy potential. One form of the explicit expressions of the damage release rates proposed by Wu et al. (2006) reads

$$\begin{aligned} Y^+ &\approx \frac{1}{2E_0}\left[\frac{2(1+\nu_0)}{3}3\bar{J}_2^+ + \frac{1-2\nu_0}{3}(\bar{I}_1^+)^2 - \nu_0\bar{I}_1^+\bar{I}_1^-\right] \\ Y^- &\approx b_0\left(\alpha\bar{I}_1^- + \sqrt{3\bar{J}_2^-}\right)^2 \end{aligned} \tag{37}$$

where $\bar{I}_1^\pm$ = first invariants of the corresponding effective stresses components, $\bar{\boldsymbol{\sigma}}^\pm$; and $\bar{J}_2^\pm$ are the second invariants of $\bar{\boldsymbol{s}}^\pm$ which are the deviatoric components of $\bar{\boldsymbol{\sigma}}^\pm$. E_0 and ν_0 = initial elastic modulus and the Poisson's ratio of the undamaged concrete; b_0 = model parameter. And the parameter α is defined as

$$\alpha = \frac{\frac{f_{bc}}{f_c} - 1}{2\frac{f_{bc}}{f_c} - 1} \tag{38}$$

where f_c = uniaxial compressive strength; and f_{bc} = biaxial compressive strength.

Using the test results of uniaxial tension and compression, the energy equivalent strain proposed by Li and Ren (2009) is directly connected with the damage release rate

$$\begin{aligned} \varepsilon_{eq}^{e+} &= \sqrt{\frac{2Y^+}{E_0}} \\ \varepsilon_{eq}^{e-} &= \frac{1}{E_0(1-\alpha)}\sqrt{Y^-} \end{aligned} \tag{39}$$

Then, the damage evolution is defined as the function of the energy equivalent strain

$$d^\pm = g^\pm(r_e^\pm), \qquad r_e^\pm = \max_{\tau\in[0,t]}(\varepsilon_{eq}^{e\pm}) \tag{40}$$

where the damage thresholds, $r_e^\pm$, are the maximum values of the energy equivalent strain, $\varepsilon_{eq}^{e\pm}$, throughout the entire loading process.

Plasticity Evolution

A multivariable phenomenological plastic model proposed by Ren et al. (2015) is adopted to consider the different plastic evolutions under tensile and compressive stress states. The total plastic strain rate is divided into the tensile (positive) and compressive (negative) components

$$\dot{\varepsilon}^p = \dot{\varepsilon}^{p+} + \dot{\varepsilon}^{p-} \tag{41}$$

where the tensile plastic strain rate, $\dot{\varepsilon}^{p+}$, and the compressive plastic strain rate, $\dot{\varepsilon}^{p-}$, read

$$\begin{aligned} \dot{\varepsilon}^{p+} &= f_p^+\dot{\varepsilon}^{e+} = f_p^+\mathbb{E}_0^{-1}:\dot{\bar{\boldsymbol{\sigma}}}^+ \\ \dot{\varepsilon}^{p-} &= f_p^-\dot{\varepsilon}^{e-} = f_p^-\mathbb{E}_0^{-1}:\dot{\bar{\boldsymbol{\sigma}}}^- \end{aligned} \tag{42}$$

The plastic functions, $f_p^\pm$, are defined as the effect of damage on the plastic strain

$$f_p^\pm = f_p^\pm(\dot{d}^\pm, d^\pm) = H(\dot{d}^\pm)\xi_p^\pm(d^\pm)^{n_p^\pm} \tag{43}$$

where $\xi_p^\pm$ and $n_p^\pm$ are plasticity-related parameters which need to be identified from the experimental data.

J. Eng. Mech., 2020, 146(5): 04020027

Downloaded from ascelibrary.org by University of Houston on 08/11/20. Copyright ASCE. For personal use only; all rights reserved.

The rate forms of plastic stress components are expressed as follows:

$$\dot{\sigma}^{p+} = \mathbb{E}_0 : \dot{\varepsilon}^{p+} = H(\dot{d}^+)\xi_p^+ (d^+)^{n_p^+} \dot{\tilde{\boldsymbol{\sigma}}}^+$$
$$\dot{\sigma}^{p-} = \mathbb{E}_0 : \dot{\varepsilon}^{p-} = H(\dot{d}^-)\xi_p^- (d^-)^{n_p^-} \dot{\tilde{\boldsymbol{\sigma}}}^- \quad (44)$$

Appendix II. The ACI Model

The ACI model assumes a linear creep relationship to predict creep behavior of concrete. The creep coefficient defined as the ratio of creep strain to initial strain is formulated as follows:

$$\varphi(t, t_0) = \frac{(t - t_0)^a}{b + (t - t_0)^a} \varphi_\infty \quad (45)$$

where t = current age of concrete, in days; t_0 = age of concrete at loading, in days; φ_∞ = ultimate creep coefficient, and the parameters a and b define the shape and size of the time-related part.

The ultimate creep coefficient is defined as follows:

$$\varphi_\infty = 2.35\gamma_c \quad (46)$$

where γ_c represents the product of several applicable correction factors, i.e., type of cement, type and period of curing, characteristic compressive strength, age at loading, ambient relative humidity, and temperature.

Data Availability Statement

Some or all data, models, or code that support the findings of this study are available from the corresponding author upon reasonable request.

Acknowledgments

This work was supported by the National Natural Science Foundation of China (Grant Nos. 51678439 and 51538010).

References

ACI (American Concrete Institute). 2008. *Guide for modeling and calculating shrinkage and creep in hardened concrete*. ACI 209.2R. Farmington Hills, MI: ACI.

Bažant, Z. P., and S. Baweja. 2000. "Creep and shrinkage prediction model for analysis and design of concrete structures: Model B3." In *Proc., Adam Neville Symp.: Creep and Shrinkage—Structural Design Effects, ACI SP-194* edited by A. Al-Manaseer, 1–84. Farmington Hills, MI: American Concrete Institute.

Bažant, Z. P., and J. C. Chern. 1985. "Strain softening with creep and exponential algorithm." *J. Eng. Mech.* 111 (3): 391–415. https://doi.org/10.1061/(ASCE)0733-9399(1985)111:3(391).

Bažant, Z. P., and W. P. Murphy. 1995. "Creep and shrinkage prediction model for analysis and design of concrete structures-Model B3." *Matériaux Constructions* 28 (180): 357–365.

Bažant, Z. P., and J. Planas. 1997. *Fracture and size effect in concrete and other quasibrittle materials*. New York: CRC Press.

Bažant, Z. P., and S. Prasannan. 1989. "Solidification theory for concrete creep. I: Formulation." *J. Eng. Mech.* 115 (8): 1691–1703. https://doi.org/10.1061/(ASCE)0733-9399(1989)115:8(1691).

Benboudjema, F., and J. M. Torrenti. 2008. "Early-age behaviour of concrete nuclear containments." *Nucl. Eng.* 238 (10): 2495–2506. https://doi.org/10.1016/j.nucengdes.2008.04.009.

Carol, I., and J. Murcia. 1989. "A model for the non-linear time-dependent behaviour of concrete in compression based on a Maxwell chain with exponential algorithm." *Mater. Struct.* 22 (3): 176–184. https://doi.org/10.1007/BF02472185.

Challamel, N., C. Lanos, and C. Casandjian. 2005. "Creep damage modelling for quasi-brittle materials." *Eur. J. Mech. A-Solid* 24 (4): 593–613. https://doi.org/10.1016/j.euromechsol.2005.05.003.

Clarke, G. S. 1987. "Long-term deflection of reinforced concrete flexural elements." M.Sc. thesis, Graduate Program in Civil and Environmental Engineering, Univ. of the Witwatersrand.

fib (International Federation for Structural Concrete). 2010. *Model code 2010*, 132–139. Lausanne, Switzerland: fib.

Freudenthal, A. M., and F. Roll. 1958. "Creep and creep recovery of concrete under high compressive stress." *ACI J. Proc.* 54 (6): 1111–1142.

Gardner, N. J. 2000. "Design provisions for shrinkage and creep of concrete." *ACI Spec. Publ.* 194: 101–133.

Gardner, N. J., and M. J. Lockman. 2001. "Design provisions of shrinkage and creep of normal-strength concrete." *ACI Mater. J.* 98 (2): 159–167.

Gardner, N. J., and J. W. Zhao. 1993. "Creep and shrinkage revisited." *ACI Mater. J.* 90 (3): 236–246.

Geng, Y. M., W. Y. Liu, and C. H. Xia. 2013 "An experimental study on creep of high performance concrete." [In Chinese.] *Sichuan Build. Sci.* 39 (01): 169–173.

Ju, J. W. 1989. "On energy-based coupled elastoplastic damage theories: Constitutive modeling and computational aspects." *Int. J. Solids Struct.* 25 (7): 803–833. https://doi.org/10.1016/0020-7683(89)90015-2.

Lemaitre, J., and J. L. Chaboche. 1990. *Mechanics of solid materials*. London: Cambridge University Press.

Li, J., and X. D. Ren. 2009. "Stochastic damage model for concrete based on energy equivalent strain." *Int. J. Solids Struct.* 46 (11–12): 2407–2419. https://doi.org/10.1016/j.ijsolstr.2009.01.024.

Li, Z. X. 1994. "Effective creep Poisson's ratio for damaged concrete." *Int. J. Fract.* 176 (2): 189–194. https://doi.org/10.1007/s10704-012-9744-9.

Luzio, G. D., and G. Cusatis. 2013. "Solidification–microprestress–microplane (SMM) theory for concrete at early age: Theory, validation and application." *Int. J. Solids Struct.* 50 (6): 957–975. https://doi.org/10.1016/j.ijsolstr.2012.11.022.

Mazzotti, C., and M. Savoia. 2003. "Nonlinear creep damage model for concrete under uniaxial compression." *J. Eng. Mech.* 129 (9): 1065–1075. https://doi.org/10.1061/(ASCE)0733-9399(2003)129:9(1065).

Neville, A. M. 1971. *Creep of concrete: Plain, reinforced, and prestressed*. Amsterdam, Netherlands: North-Holland Pub Co.

Omar, M., A. Loukili, G. Pijaudier-Cabot, and Y. Le Pape. 2009. "Creep-damage coupled effects: Experimental investigation on bending beams with various sizes." *J. Mater. Civ. Eng.* 21 (2): 65–72. https://doi.org/10.1061/(ASCE)0899-1561(2009)21:2(65).

Omar, M., G. Pijaudier-Cabot, and A. Loukili. 2003. "Numerical models for coupling creep and fracture of concrete structures." In *Proc., Computational Modelling of Concrete Structures Euro-Conf.*, 531–539. Boca Raton, FL: CRC Press.

Proust, E., and G. Pons. 2001. "Macroscopic and microscopic behavior of self-compacting concrete creep and shrinkage." *Proc. Concreep* 6: 569–574.

Rabier, P. J. 1989. "Some remarks on damage theory." *Int. J. Eng. Sci.* 27 (1): 29–54. https://doi.org/10.1016/0020-7225(89)90166-3.

Ren, X. D., S. J. Zeng, and J. Li. 2015. "A rate-dependent stochastic damage–plasticity model for quasi-brittle materials." *Comput. Mech.* 55 (2): 267–285. https://doi.org/10.1007/s00466-014-1100-7.

Reviron, N., F. Benboudjema, J. M. Torrenti, G. Nahas, and A. Millard. 2007. "Coupling between creep and cracking in tension." In *Proc., 6th Int. Conf. on Fracture Mechanics of Concrete and Concrete Structures*. Catania, Italy: RILEM.

Roll, F. 1964. Vol. 9 of *Long-time creep-recovery of highly stressed concrete cylinders*, 95–114. Detroit: American Concrete Institute.

Ruiz, M. F., A. Muttoni, and P. G. Gambarova. 2007. "Relationship between nonlinear creep and cracking of concrete under uniaxial compression." *J. Adv. Concr. Technol.* 5 (3): 383–393. https://doi.org/10.3151/jact.5.383.

Simo, J. C., and T. J. Hughes. 2006. *Computational inelasticity*. New York: Springer.

Downloaded from ascelibrary.org by University of Houston on 08/11/20. Copyright ASCE. For personal use only; all rights reserved.

Simo, J. C., and J. W. Ju. 1987a. "Strain and stress-based continuum damage. Model. Part I: Formulation." *Int. J. Solids Struct.* 23 (7): 821–840. https://doi.org/10.1016/0020-7683(87)90083-7.

Simo, J. C., and J. W. Ju. 1987b. "Strain- and stress-based continuum damage models. Part II: Computational aspects." *Int. J. Solids Struct.* 23 (7): 841–869. https://doi.org/10.1016/0020-7683(87)90084-9.

Voyiadjis, G. Z., and T. M. Abu-Lebdeh. 1994. "Plasticity model for concrete using the bounding surface concept." *Int. J. Plast.* 10 (1): 1–21. https://doi.org/10.1016/0749-6419(94)90051-5.

Voyiadjis, G. Z., and P. I. Kattan. 2009. "A comparative study of damage variables in continuum damage mechanics." *Int. J. Damage Mech.* 18 (4): 315–340. https://doi.org/10.1177/1056789508097546.

Voyiadjis, G. Z., Z. N. Taqieddin, and P. I. Kattan. 2008. "Anisotropic damage–plasticity model for concrete." *Int. J. Plast.* 24 (10): 1946–1965. https://doi.org/10.1016/j.ijplas.2008.04.002.

Wu, J. Y., J. Li, and R. Faria. 2006. "An energy release rate-based plastic-damage model for concrete." *Int. J. Solids Struct.* 43 (3–4): 583–612. https://doi.org/10.1016/j.ijsolstr.2005.05.038.

Downloaded from ascelibrary.org by University of Houston on 08/11/20. Copyright ASCE. For personal use only; all rights reserved.